Journal of Materials Chemistry C

ROYAL SOCIETY OF CHEMISTRY

PAPER

View Article Online
View Journal | View Issue

Cite this: J. Mater. Chem. C, 2022, 10, 8776

$Mg(H_2O)_6[(IO_2(OH))_2(IO_3)]_2$: a new iodate with a very large band gap and optical anisotropy†

Yang Li and Kang Min Ok *

Received 21st April 2022,
Accepted 9th May 2022

DOI: 10.1039/d2tc01638a

rsc.li/materials-c

Centimeter-sized large crystals of a new magnesium iodate, $Mg(H_2O)_6[(IO_2(OH))_2(IO_3)]_2$, have been successfully grown by a facile aqua-solution method. The title compound exhibits an interesting structural feature, namely, $[(IO_2(OH))_2(IO_3)]^-$ pseudo-chains interacting with $[Mg(H_2O)_6]^{2+}$ octahedra *via* the hydrogen bonds. $Mg(H_2O)_6[(IO_2(OH))_2(IO_3)]_2$ possessing a large band gap of 4.10 eV exhibits the largest birefringence (0.230 @1064 nm) among the iodate systems containing alkali, alkaline earth, or rare earth metal cations, indicating that the compound is a promising birefringent material that could be applied in the ultraviolet region. The electron density difference map indicates that the great birefringence of the material is attributed to the synergistic effect of the iodate groups and the coordinated water molecules. This work also successfully provides a new method for functional crystals with large birefringence *via* a facile aqua-solution method.

Introduction

Iodate is an important family of multifunctional materials that can be applied to various industrial processes such as photonics, optical communications, medical lasers, and data storage fields.[1–4] Many functional iodate materials with macroscopic noncentrosymmetric structures revealing interesting properties have been discovered with the aid of stereochemically active lone pair electrons.[5] In addition, iodates can exhibit broad transmittance windows up to mid-infrared regions, and high-quality large crystals of iodates are often easily grown. Thus, a number of famous nonlinear optical (NLO) materials such as α-HIO_3, α-$LiIO_3$, and KIO_3 as well as newly designed iodates satisfying the ever-growing requirements of the industry have been continuously discovered in the past several decades.[6–26] In general, basic building units observed from the metal iodates are IO_3 and IO_4 polyhedra. The units are also able to generate dimers, trimers, and even more complicated groups such as I_2O_5, I_3O_8, I_4O_{11}, I_3O_9, *etc.*[3,14,26] Further extension *via* strong intermolecular interactions can also result in a variety of iodate groups with various frameworks.[26] The variable iodate building blocks not only enrich the structural chemistry, but also provide many interesting compounds with outstanding optical properties including a large SHG response and birefringence.[27–36]

It is well known that birefringence is an important parameter for viable NLO and birefringent materials. To design viable materials with large birefringence, several building blocks with large polarizability and anisotropy such as the coplanar groups (BO_3, B_3O_6, $C_3O_3N_3$, *etc.*), lone pair cations (Pb^{2+}, Bi^{3+}, I^{5+}, *etc.*), and d^0 transition metal cations (Nb^{5+}, Mo^{6+}, *etc.*) with second-order Jahn–Teller effect have been recommended.[23,37,38] The higher density and the optimal arrangement of the building blocks through suitable interactions such as hydrogen bonds in the structures also could boost the optical anisotropy of the target compounds. Guided by the above-mentioned strategy, a variety of promising NLO and birefringent crystals have been designed thus far. Specifically, several iodates with large birefringence such as $Bi(IO_3)F_2$ and $Ba_2[VO_2F_2(IO_3)_2]IO_3$ have been constructed by introducing lone pair cations or d^0 transition metal cations.[8,11] Unfortunately, however, most of the materials possess quite narrow band gaps. Thus, to broaden the band gaps, iodates containing main group metal cations such as $Ba_2[GaF_4(IO_3)_2]IO_3$, $LiGaF_2(IO_3)_2$, and $Ba[InF_3(IO_3)_2]$ have been prepared, where the combination of iodates and distorted octahedra groups was proven to be an effective way to design interesting birefringent materials with large band gaps.[39–41] In this paper, we have explored the Mg^{2+} cation containing iodate system to discover new birefringent materials. By doing so, a new magnesium iodate, $Mg(H_2O)_6[(IO_2(OH))_2(IO_3)]_2$, has been successfully obtained *via* the facile aqua-solution method at room temperature. Hydrogen bonding interactions between $[Mg(H_2O)_6]^{2+}$ octahedra and iodate groups could generate a novel structural feature.[42] In addition, the coordinated aqua ligands may also be expected to contribute to improving the birefringence.[43]

Department of Chemistry, Sogang University, Seoul 04107, Republic of Korea. E-mail: kmok@sogang.ac.kr

† Electronic supplementary information (ESI) available: Crystallographic data, IR spectrum, TGA diagram, band structure, and electron density difference map of $Mg(H_2O)_6[(IO_2(OH))_2(IO_3)]_2$. CCDC 2167789. For ESI and crystallographic data in CIF or other electronic format see DOI: https://doi.org/10.1039/d2tc01638a

Experimental section

Reagents

$Mg(NO_3)_2{\cdot}6H_2O$ (Yakuri, 99%) and HIO_3 (Alfa, 99%) were used as reagents as received.

Single crystal growth

Single crystals of $Mg(H_2O)_6[(IO_2(OH))_2(IO_3)]_2$ were grown by the aqua-solution method at room temperature. $Mg(NO_3)_2{\cdot}6H_2O$ (1 mmol), HIO_3 (3 mmol), and 5 mL of distilled water were mixed in a dish and thoroughly stirred using a glass rod to dissolve the reagents. Transparent needle like crystals were grown for a week in 75% yield based on $Mg(NO_3)_2{\cdot}6H_2O$ once the water slowly evaporated at room temperature.

Measurements

The single crystal X-ray diffraction data of $Mg(H_2O)_6[(IO_2(OH))_2(IO_3)]_2$ were collected at room temperature *via* a Bruker D8 QUEST diffractometer with a graphite-monochromated MoKα radiation source (λ = 0.71073 Å) at the Advanced Bio-Interface Core Research Facility, Sogang University. Data reduction and absorption correction were made using the SAINT and SADABS programs, respectively.[44,45] The crystal structure was solved using the OLEX2 package.[46] The program PLATON was applied to validate if any higher symmetry is missing there.[47] Crystallographic data, structure refinement information, atomic coordinates, equivalent isotropic displacement parameters, and bond valence sums of all atoms except for H atoms are listed in the ESI.† Powder X-ray diffraction data were collected on a Rigaku Mini Flex 600 diffractometer using Cu Kα (λ = 1.5406 Å) radiation with 40 kV and 15 mA at room temperature. The well-ground polycrystalline sample mounted on a sample holder was scanned in the 2θ range of 5–70° at a scan speed of 20° min^{-1} and a scan step width of 0.02°. The measured diffraction pattern of the title compound matched well with the calculated data generated from single crystal X-ray diffraction (Fig. 1).

Infrared (IR) spectra were recorded on a Thermo Scientific Nicolet iS50 FT-IR spectrometer in the spectral range of 500 to 4000 cm^{-1}. The ground sample was made to be in contact with the diamond attenuated-total-reflectance crystal.

Ultraviolet-visible (UV-vis) diffuse-reflectance spectra for $Mg(H_2O)_6[(IO_2(OH))_2(IO_3)]_2$ were obtained on a Lambda 1050 scan UV-vis-NIR spectrophotometer over the spectral range of 200–700 nm at room temperature. The reflection spectra were converted to the absorbance data using the Kubelka–Munk function.[48]

Thermogravimetric analysis (TGA) was performed using a SCINCO TGA-N 1000 thermal analyzer. The ground polycrystalline sample was loaded into an alumina crucible and heated to 900 °C at a rate of 10 °C min^{-1} under flowing air. Differential scanning calorimetry data were also obtained on a TA DSC-Q2000 from room temperature to 350 °C at a heating rate of 10 °C min^{-1} under flowing nitrogen.

First-principles density functional theory calculations were performed using the CASTEP package.[49] The band structure, density of states, and the optical properties were calculated by using the Perdew–Burke–Ernzerhof generalized gradient approximation (GGA).[50–52] A plane-wave cut-off energy of 925 eV was chosen. To obtain a good convergence of electronic structures and optical properties, the dense *k*-point sampling less than 0.03 $Å^{-1}$ was adopted.

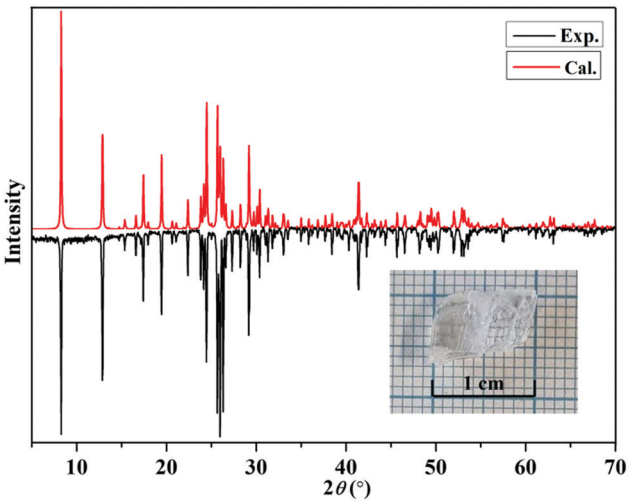

Fig. 1 Experimental and calculated powder XRD patterns of $Mg(H_2O)_6[(IO_2(OH))_2(IO_3)]_2$. Inset: The picture of an as-grown large crystal.

Results and discussion

Crystal structure

$Mg(H_2O)_6[(IO_2(OH))_2(IO_3)]_2$ crystallizes in the monoclinic space group, $P2_1/c$. In an asymmetric unit, one $[Mg(H_2O)_6]^{2+}$, four $IO_2(OH)$, and two IO_3 units exist (Fig. S1, ESI†). The unique Mg^{2+} cation is coordinated by six H_2O molecules to form the $[Mg(H_2O)_6]^{2+}$ octahedron, in which the Mg–O distances are in the range of 2.036–2.110 Å. While both I(1) and I(3) are linked with two O atoms and one OH^- to form $IO_2(OH)$ groups, I(2) is connected by three O atoms to form the IO_3 trigonal pyramid. The distances between I and O atoms observed in $IO_2(OH)$ and IO_3 groups range from 1.780 to 1.913 Å. Long atom contacts such as I(1)···O(7) [2.453 Å], I(2)···O(9) [2.611 Å], and I(3)···O(11) [2.461 Å] are also observed. Considering those longer interactions, $[(IO_2(OH))_2(IO_3)]^-$ infinite tubules that are running along the *c*-axis are monitored (Fig. 2a and b). Finally, hydrogen bonding interactions between the $[Mg(H_2O)_6]^{2+}$ octahedra and $[(IO_2(OH))_2(IO_3)]^-$ tubules complete the whole structure of $Mg(H_2O)_6[(IO_2(OH))_2(IO_3)]_2$ (Fig. 2c and d). Bond valence sum calculations on the Mg^{2+}, I^{5+}, OH^-, and O^{2-} result in values of 2.14, 5.12–5.23, 1.28–1.34, and 1.68–2.03, respectively.[42,53]

IR spectroscopy

The IR spectrum of the reported compound reveals vibrations occurring from Mg–O, I–O, and O–H bonds (Fig. S2, ESI†). Weak bands at *ca.* 1413 and 823 cm^{-1} are associated with the Mg–O bonds.[54,55] The bands found at *ca.* 779, 750, 711, 552,

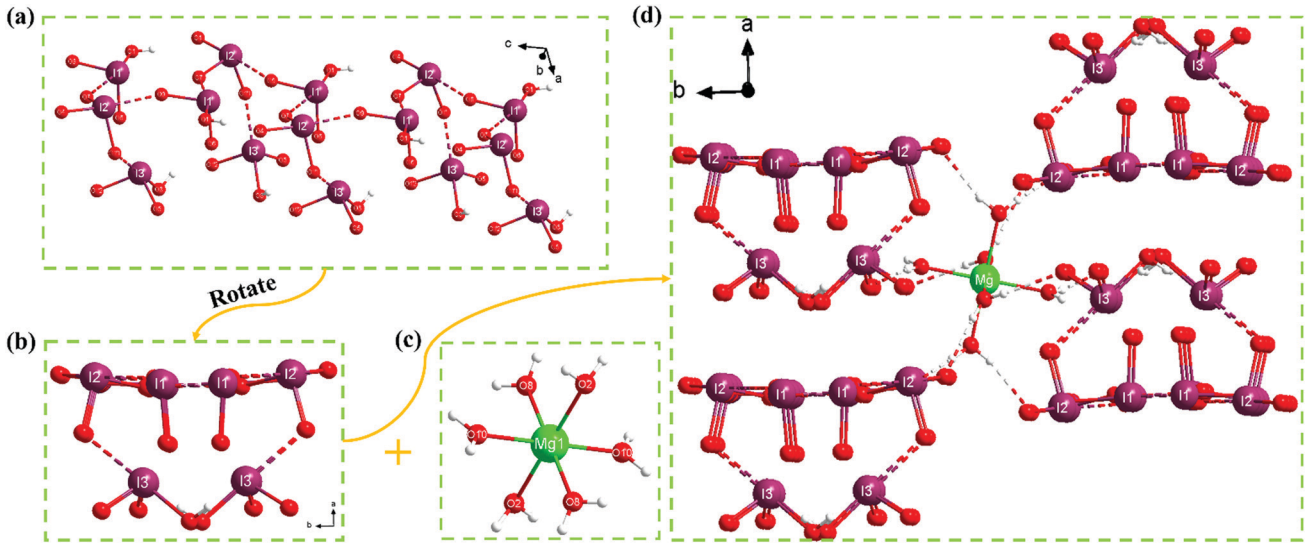

Fig. 2 $[(IO_2(OH))_2(IO_3)]^-$ infinite tubules viewed along the (a) *b*-axis and (b) *c*-axis, and the (c) $[Mg(H_2O)_6]^{2+}$ octahedron in $Mg(H_2O)_6[(IO_2(OH))_2(IO_3)]_2$. (d) Hydrogen bonding interactions between the $[Mg(H_2O)_6]^{2+}$ octahedron and $[(IO_2(OH))_2(IO_3)]^-$ infinite tubules.

525, and 517 cm^{-1} are attributable to the I–O vibrations.[32,42,56] The peaks occurring at *ca.* 3365 and 1632 cm^{-1} are responsible for O–H bonds.[42,43]

UV-vis diffuse reflectance spectroscopy

The UV-vis diffuse reflectance spectrum suggests that $Mg(H_2O)_6[(IO_2(OH))_2(IO_3)]_2$ possesses a short cut-off edge of *ca.* 262 nm (Fig. 3). The cut-off edge is smaller than most iodates containing alkali or alkaline earth, lone pair, and rare earth metal cations such as $LiIO_3$ (280 nm), $RbIO_2F_2$ (295 nm), $Ba[FeF_4(IO_3)]$ (281 nm), $Bi_2(IO_4)(IO_3)_3$ (376 nm), and $Ce(IO_3)_2F_2$ (452 nm).[10,12,33,57,58] Hence, the reported iodate with a broad band gap could be a potential birefringent crystal that can be applied in the UV region.

Thermal analysis

As seen in the TGA diagram, $Mg(H_2O)_6[(IO_2(OH))_2(IO_3)]_2$ reveals three thermal decomposition steps (Fig. S3, ESI†). Initially, the title compound exhibits a weight loss of 12.5% between 84 and 227 °C attributed to the loss of eight H_2O molecules from $Mg(H_2O)_6^{2+}$ and $IO_2(OH)$ groups, which are in agreement with the endothermic peaks occurring at 86 to 204 °C in the DSC diagram. And then, 2 equivalents of I_2 and 5 equivalents of O_2 are lost at *ca.* 344 and 433 °C, calculated (experimental): 56.3% (56.0%). Finally, I_2 and 5/2 O_2 are released between 540 and 710 °C, calculated (experimental): 27.8% (Exp. 27.6%).

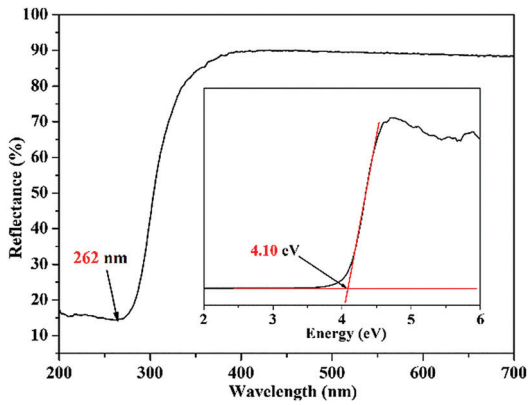

Fig. 3 UV-vis diffuse reflectance spectrum of $Mg(H_2O)_6[(IO_2(OH))_2(IO_3)]_2$.

Electronic structure calculations

The electronic structure calculations predict a band gap of 2.83 eV for $Mg(H_2O)_6[(IO_2(OH))_2(IO_3)]_2$, which is significantly smaller than the experimental value of 4.10 eV (Fig. 4 and Fig. S4, ESI†). The underestimating tendency of the band gap energy obtained by the electronic band structure calculations from the GGA functional attributable to the PBE exchange-correlation energy has been well documented.[59,60] However, the calculations are still useful in identifying important orbital interactions with a reliable trend. As seen from the band structure, the title compound belongs to an indirect band gap compound because the valence band maximum and the conduction band minimum are located at different points. The conduction band minimum and the valence band maximum are dominated by the I 5p and O 2p orbitals, respectively, with small number of mixing from the I 5s orbitals (Fig. 4). Thus, the IO_3 and $IO_2(OH)$ groups occupying the highest valence band and the lowest conduction band mainly determine the optical properties of $Mg(H_2O)_6[(IO_2(OH))_2(IO_3)]_2$.

To confirm the longer interactions between the I and O groups (bond lengths ≥ 2.46 Å), the electron localization function was calculated (Fig. 5a).[26,61] The obvious gaps between the I1···O7, I2···O9, and I3···O11 strongly suggest that the interactions between them are intermolecular interactions rather than the normal covalent I–O bonds in these structures.

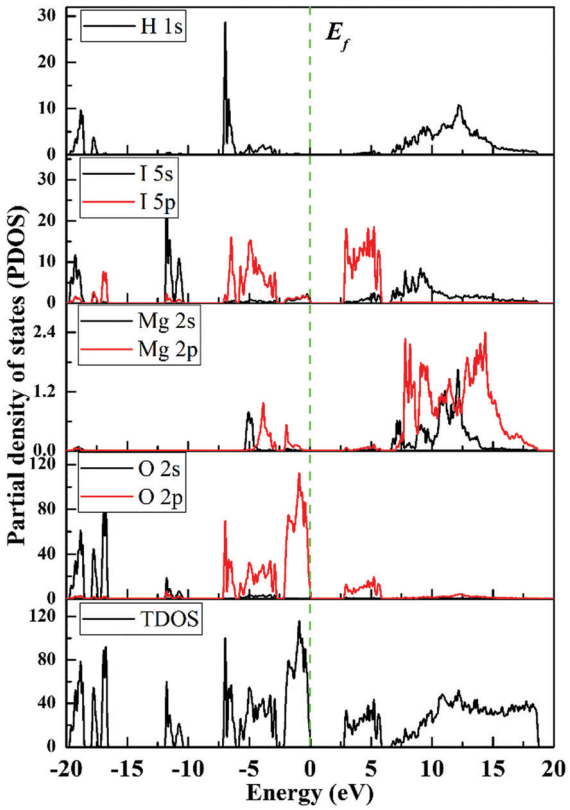

Fig. 4 Density of states for $Mg(H_2O)_6[(IO_2(OH))_2(IO_3)]_2$.

Birefringence

Based on the plot of calculated birefringence in Fig. 5b, $Mg(H_2O)_6[(IO_2(OH))_2(IO_3)]_2$ possesses a very large birefringence of 0.230 @1064 nm, which is much larger than those of most reported iodates. In fact, this value is the largest one among the iodate systems containing alkali, alkaline earth, or rare earth metal cations (ESI†). To further investigate the source of the birefringence, the electron density difference map was calculated (Fig. S5, ESI†). By doing so, we found that the strong covalent I–O and O–H bonds existing in IO_3, $IO_2(OH)$, and H_2O should contribute to the large birefringence of $Mg(H_2O)_6[(IO_2(OH))_2(IO_3)]_2$. Once we substitute Mg^{2+} for the large Ba^{2+} cation and remove In^{3+} in $Ba[InF_3(IO_3)_2]$, we were able to enhance the density of I–O groups from 4.9×10^{-3} Å^{-3} to 10.8×10^{-3} Å^{-3}. Although $Mg(H_2O)_6[(IO_2(OH))_2(IO_3)]_2$ consists of a weaker distortive octahedra (Δd = 0.15), the compound still possesses a larger birefringence than those of $Ba[InF_3(IO_3)_2]$ (0.172 @1064 nm; Δd (InO_2F_4) = 0.35) and $LiGaF_2(IO_3)_2$ (0.181 @1064 nm; Δd(GaF_2O_4) = 0.25). The band gap and birefringence for the reported typical iodates are listed in Table 1. As shown in Table 1, $Mg(H_2O)_6[(IO_2(OH))_2(IO_3)]_2$ exhibits a good balance between the band gap and birefringence. Even compared with several commercial birefringent crystals such as $LiNbO_3$ (0.0836 @633 nm), α-BaB_2O_4 (0.1222 @532 nm), and $CaCO_3$ (0.171 @633 nm), $Mg(H_2O)_6[(IO_2(OH))_2(IO_3)]_2$ exhibits a very attractive birefringence that can be applied to a promising UV birefringent crystal.[63–65]

Table 1 Band gap and birefringence (Δn @1064 nm) for typical iodates

Compound	band gap (eV)	Δn @1064 nm	Ref.
$RbIO_3$	4.0	0.063	10
YI_5O_{14}	3.82	0.091	62
GdI_5O_{14}	4.07	0.092	62
α-AgI_3O_8	3.78	0.208	27
β-AgI_3O_8	3.59	0.210	27
NaI_3O_8	3.93	0.213	26
$Ba_2[FeF_4(IO_3)_2]IO_3$	3.9	0.125	57
$LiGaF_2(IO_3)_2$	4.33	0.181	40
$Ba[InF_3(IO_3)_2]$	4.35	0.172	41
$Bi(IO_3)F_2$	3.97	0.209	8
$Ce(IO_3)_4$	2.17	0.039 (@546 nm)	58
$Mg(H_2O)_6[(IO_2(OH))_2(IO_3)]_2$	4.10	0.230	This work

Conclusion

Crystals of a new magnesium iodate, $Mg(H_2O)_6[(IO_2(OH))_2(IO_3)]_2$, consisting of $Mg(H_2O)_6$, IO_3, and $IO_2(OH)$ groups have been grown

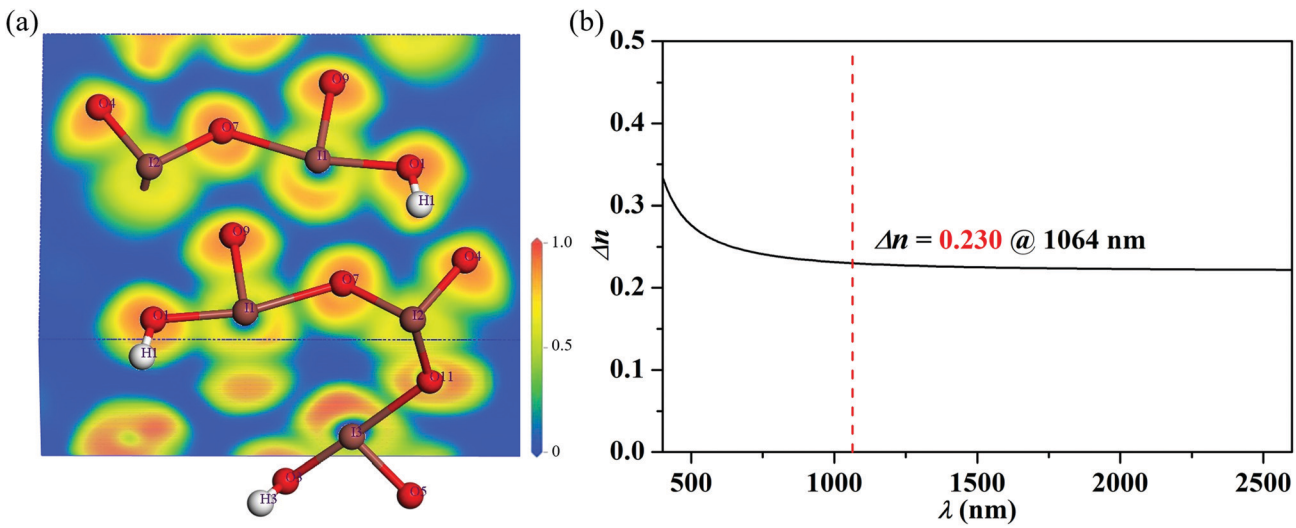

Fig. 5 (a) Electron localization function diagram and (b) calculated birefringence for $Mg(H_2O)_6[(IO_2(OH))_2(IO_3)]_2$.

via an aqua-solution method. The reported material reveals an interesting pseudo-3D structural feature that is composed of $[Mg(H_2O)_6]^{2+}$ octahedra and $[(IO_2(OH))_2(IO_3)]^-$ tubules through hydrogen bonding interactions. The compound possesses a large band gap of 4.10 eV and a short UV cut-off edge of 262 nm. Interestingly, the synergistic effect of distorted $[Mg(H_2O)_6]^{2+}$, IO_3, and $IO_2(OH)$ groups resulted in a very large calculated birefringence of 0.230@1064 nm. $Mg(H_2O)_6[(IO_2(OH))_2(IO_3)]_2$ maintains a good balance between the band gap and birefringence, which successfully enables the material as a potential birefringent crystal in the UV region. We are in the process of introducing F^- anions into a similar framework structure to shorten the UV cut-off edge while maintaining the large birefringence.

Conflicts of interest

There are no conflicts to declare.

Acknowledgements

This research was supported by the National Research Foundation of Korea (NRF) funded by the Ministry of Science and ICT (Grant No. 2018R1A5A1025208 and 2019R1A2C3005530).

Notes and references

1 P. S. Halasyamani and K. R. Poeppelmeier, Noncentrosymmetric Oxides, *Chem. Mater.*, 1998, **10**, 2753–2769.
2 H. Y. Chang, S. H. Kim, P. S. Halasyamani and K. M. Ok, Alignment of lone pairs in a new polar material: Synthesis, characterization, and functional properties of $Li_2Ti(IO_3)_6$, *J. Am. Chem. Soc.*, 2009, **131**, 2426–2427.
3 R. E. Sykora, K. M. Ok, P. S. Halasyamani and T. E. Albrecht-Schmitt, Structural modulation of molybdenyl iodate architectures by alkali metal cations in $AMoO_3(IO_3)$ (A = K, Rb, Cs): A facile route to new polar materials with large SHG responses, *J. Am. Chem. Soc.*, 2002, **124**, 1951–1957.
4 C. L. Hu and J. G. Mao, Recent advances on second-order NLO materials based on metal iodates, *Coord. Chem. Rev.*, 2015, **288**, 1–17.
5 C. T. Chen, Y. C. Wu and R. K. Li, The anionic group theory of the non-linear optical effect and its applications in the development of new high-quality NLO crystals in the borate series, *Int. Rev. Phys. Chem.*, 1988, **8**, 65–91.
6 X. L. Chen and K. M. Ok, Recent Advances in Oxide-based Nonlinear Optical Materials with Wide Infrared Transparency Beyond 6 μm, *Chem. – Asian J.*, 2020, **15**, 3709–3716.
7 M. Zhang, C. Hu, T. Abudouwufu, Z. H. Yang and S. L. Pan, Functional Materials Design via Structural Regulation Originated from Ions Introduction: A Study Case in Cesium Iodate System, *Chem. Mater.*, 2018, **30**, 1136–1145.
8 F. F. Mao, C. L. Hu, X. Xu, D. Yan, B. P. Yang and J. G. Mao, $Bi(IO_3)F_2$: The First Metal Iodate Fluoride with a Very Strong Second Harmonic Generation Effect, *Angew. Chem., Int. Ed.*, 2017, **56**, 2151–2155.
9 H. Fan, C. S. Lin, K. C. Chen, G. Peng, B. X. Li, G. Zhang, X. F. Long and N. Ye, $(NH_4)Bi_2(IO_3)_2F_5$: An Unusual Ammonium-containing Metal Iodate Fluoride Showing Strong Second Harmonic Generation (SHG) Response and Thermochromic Behavior, *Angew. Chem., Int. Ed.*, 2020, **59**, 5268–5272.
10 Q. Wu, H. M. Liu, F. C. Jiang, L. Kang, L. Yang, Z. S. Lin, Z. G. Hu, X. G. Chen, X. G. Meng and J. G. Qin, $RbIO_3$ and $RbIO_2F_2$: Two Promising Nonlinear Optical Materials in Mid-IR Region and Influence of Partially Replacing Oxygen with Fluorine for Improving Laser Damage Threshold, *Chem. Mater.*, 2016, **28**, 1413–1418.
11 H. W. Yu, M. L. Nisbet and K. R. Poeppelmeier, Assisting the Effective Design of Polar Iodates with Early Transition-Metal Oxide Fluoride Anions, *J. Am. Chem. Soc.*, 2018, **140**, 8868–8876.
12 V. G. Dmitriev, G. G. Gurzadyan and D. N. Nikogosyan, *Handbook of nonlinear optical crystals*, Springer, 2013.
13 Z. G. Xia and K. R. Poeppelmeier, Chemistry-Inspired Adaptable Framework Structures, *Acc. Chem. Res.*, 2017, **50**, 1222–1230.
14 J. Chen, C. L. Hu, F. Kong and J. G. Mao, High-Performance Second-Harmonic-Generation (SHG) Materials: New Developments and New Strategies, *Acc. Chem. Res.*, 2021, **54**, 2775–2783.
15 K. M. Ok, Toward the Rational Design of Novel Noncentrosymmetric Materials: Factors Influencing the Framework Structures, *Acc. Chem. Res.*, 2016, **49**, 2774–2785.
16 Y. Wang, B. B. Zhang, Z. H. Yang and S. L. Pan, Cation-Tuned Synthesis of Fluorooxoborates: Approaching the Optimal Deep-Ultraviolet Nonlinear Optical Materials, *Angew. Chem., Int. Ed.*, 2018, **130**, 2172–2176.
17 G. Q. Shi, Y. Wang, F. F. Zhang, B. B. Zhang, Z. H. Yang, X. L. Hou, S. L. Pan and K. R. Poeppelmeier, Finding the Next Deep-Ultraviolet Nonlinear Optical Material: $NH_4B_4O_6F$, *J. Am. Chem. Soc.*, 2017, **139**, 10645–10648.
18 B. B. Zhang, G. Q. Shi, Z. H. Yang, F. F. Zhang and S. L. Pan, Fluorooxoborates: Beryllium-Free Deep-Ultraviolet Nonlinear Optical Materials without Layered Growth, *Angew. Chem., Int. Ed.*, 2017, **56**, 3916–3919.
19 M. Mutailipu, M. Zhang, B. B. Zhang, L. Y. Wang, Z. H. Yang, X. Zhou and S. L. Pan, $SrB_5O_7F_3$ Functionalized with $[B_5O_9F_3]^{6-}$ Chromophores: Accelerating the Rational Design of Deep-Ultraviolet Nonlinear Optical Materials, *Angew. Chem., Int. Ed.*, 2018, **130**, 6203–6207.
20 X. F. Wang, Y. Wang, B. B. Zhang, F. F. Zhang, Z. H. Yang and S. L. Pan, CsB_4O_6F: A Congruent-Melting Deep-Ultraviolet Nonlinear Optical Material by Combining Superior Functional Units, *Angew. Chem., Int. Ed.*, 2017, **56**, 14119–14123.
21 J. Lu, J. N. Yue, L. Xiong, W. K. Zhang, L. Chen and L. M. Wu, Uniform Alignment of Non-π-Conjugated Species Enhances Deep Ultraviolet Optical Nonlinearity, *J. Am. Chem. Soc.*, 2020, **141**, 8093–8097.
22 S. G. Jantz, M. Dialer, L. Bayarjargal, B. Winkler, L. van Wüllen, F. Pielnhofer, J. Brgoch, R. Weihrich and H. A. Höppe,

$Sn[B_2O_3F_2]$—The First Tin Fluorooxoborate as Possible NLO Material, *Adv. Opt. Mater.*, 2018, **6**, 10–17.

23 X. L. Chen, B. B. Zhang, F. F. Zhang, Y. Wang, M. Zhang, Z. H. Yang, K. R. Poeppelmeier and S. L. Pan, Designing an Excellent Deep-Ultraviolet Birefringent Material for Light Polarization, *J. Am. Chem. Soc.*, 2018, **140**, 16311–16319.

24 G. H. Zou, L. Huang, N. Ye, C. Lin, W. Cheng and H. Huang, $CsPbCO_3F$: A Strong Second-Harmonic Generation Material Derived from Enhancement *via* p–π Interaction, *J. Am. Chem. Soc.*, 2013, **135**, 18560–18566.

25 J. Kee and K. M. Ok, Hydrogen-Bond-Driven Synergistically Enhanced Hyperpolarizability: Chiral Coordination Polymers with Nonpolar Structures Exhibiting Unusually Strong Second-Harmonic Generation, *Angew. Chem., Int. Ed.*, 2021, **60**, 20656–20660.

26 I. Gautier-Luneau, Y. Suffren, H. Jamet and J. Pilmé, Reinterpretation of Three Crystal Structures of Alkali Oxoiodate(V) - Description of the $[I_3O_8]^-$ anion and the infinite 2D $[I_3O_8^-]_\infty$ Anion, *Z. Anorg. Allg. Chem.*, 2010, **636**, 1368–1379.

27 X. Xu, C. L. Hu, B. X. Li, B. P. Yang and J. G. Mao, α-AgI_3O_8 and β-AgI_3O_8 with Large SHG Responses: Polymerization of IO_3 Groups into the I_3O_8 Polyiodate Anion, *Chem. Mater.*, 2014, **26**, 3219–3230.

28 D. Phanon and I. Gautier-Luneau, Promising Material for Infrared Nonlinear Optics: NaI_3O_8 Salt Containing an Octaoxotriiodate(V) Anion Formed from Condensation of $[IO_3]-$ Ions, *Angew. Chem., Int. Ed.*, 2007, **46**, 8488–8491.

29 H. Y. Chang, S. H. Kim, K. M. Ok and P. S. Halasyamani, Polar or nonpolar? A^+ cation polarity control in $A_2Ti(IO_3)_6$ (A = Li, Na, K, Rb, Cs, Tl), *J. Am. Chem. Soc.*, 2009, **131**, 6865–6873.

30 K. M. Ok and P. S. Halasyamani, The Lone-Pair Cation I^{5+} in a Hexagonal Tungsten Oxide-Like Framework: Synthesis, Structure, and Second-Harmonic Generating Properties of $Cs_2I_4O_{11}$, *Angew. Chem., Int. Ed.*, 2004, **43**, 5489–5491.

31 K. M. Ok and P. S. Halasyamani, New Metal Iodates: Syntheses, Structures, and Characterizations of Noncentrosymmetric $La(IO_3)_3$ and $NaYI_4O_{12}$ and Centrosymmetric β-$Cs_2I_4O_{11}$ and $Rb_2I_6O_{15}(OH)_2{\cdot}H_2O$, *Inorg. Chem.*, 2005, **44**, 9353–9359.

32 S. D. Nguyen, J. Yeon, S. H. Kim and P. S. Halasyamani, $BiO(IO_3)$: A New Polar Iodate that Exhibits an Aurivillius-Type $(Bi_2O_2)^{2+}$ Layer and a Large SHG Response, *J. Am. Chem. Soc.*, 2011, **133**, 12422–12425.

33 Z. B. Cao, Y. C. Yue, J. Y. Yao, Z. S. Lin, R. He and Z. G. Hu, $Bi_2(IO_4)(IO_3)_3$: A New Potential Infrared Nonlinear Optical Material Containing $[IO_4]^{3-}$ Anion, *Inorg. Chem.*, 2011, **50**, 12818–12822.

34 R. E. Sykora, K. M. Ok, P. S. Halasyamani, D. M. Wells and T. E. Albrecht-Schmitt, New One-Dimensional Vanadyl Iodates: Hydrothermal Preparation, Structures, and NLO Properties of $A[VO_2(IO_3)_2]$ (A = K, Rb) and $A[(VO)_2(IO_3)_3O_2]$ ($A = NH_4$, Rb, Cs), *Chem. Mater.*, 2002, **14**, 2741–2749.

35 C. F. Sun, C. L. Hu, X. Xu, B. P. Yang and J. G. Mao, Explorations of New Second-Order Nonlinear Optical Materials in the Potassium Vanadyl Iodate System, *J. Am. Chem. Soc.*, 2011, **133**, 5561–5572.

36 C. Wu, X. X. Jiang, Z. J. Wang, L. Lin, Z. S. Lin, Z. P. Huang, X. F. Long, M. G. Humphrey and C. Zhang, Giant Optical Anisotropy in the UV-Transparent 2D Nonlinear Optical Material $Sc(IO_3)_2(NO_3)$, *Angew. Chem., Int. Ed.*, 2021, **60**, 3464–3468.

37 X. H. Dong, L. Huang, H. M. Zeng, Z. E. Lin, K. M. Ok and G. H. Zou, High-Performance Sulfate Optical Materials Exhibiting Giant Second Harmonic Generation and Large Birefringence, *Angew. Chem., Int. Ed.*, 2022, **61**, e202116790.

38 A. Tudi, S. J. Han, Z. H. Yang and S. L. Pan, Potential optical functional crystals with large birefringence: Recent advances and future prospects, *Coord. Chem. Rev.*, 2022, **459**, 214380.

39 J. Chen, C. L. Hu, F. F. Mao, J. H. Feng and J. G. Mao, A Facile Route to Nonlinear Optical Materials: Three-Site Aliovalent Substitution Involving One Cation and Two Anions, *Angew. Chem., Int. Ed.*, 2019, **58**, 2098–2102.

40 J. Chen, C. L. Hu and J. G. Mao, $LiGaF_2(IO_3)_2$: A mixed-metal gallium iodate-fluoride with large birefringence and wide band gap, *Sci. China Mater.*, 2021, **64**, 400–407.

41 X. Q. Jiang, H. P. Wu, H. W. Yu, Z. G. Hu, J. Y. Wang and Y. C. Wu, Synthesis, Structure, Characterization, and Calculation of a Noncentrosymmetric Fluorine-Containing Indium Iodate, $Ba[InF_3(IO_3)_2]$, *Cryst. Growth Des.*, 2021, **21**, 4005–4012.

42 Y. Li, J. B. Huang and H. M. Chen, Crystal growth, characterization and theoretical studies of the noncentrosymmetric compound $Al_3(IO_3)_9{\cdot}(HIO_3)_6{\cdot}18H_2O$, *J. Alloys Compd.*, 2021, **856**, 157852.

43 W. B. Cai, J. Q. Chen, S. L. Pan and Z. H. Yang, Enhancement of Band Gap and Birefringence Induced *via* π-Conjugated Chromophore with ''Tail Effect'', *Inorg. Chem. Front.*, 2022, **9**, 1224–1232.

44 *Version 7 Saint*, 60A Bruker Analytical X-Ray Instruments, Inc., Madison, WI, 2008.

45 Bruker Suite, Bruker AXS Inc., Madison, USA, 2008.

46 O. V. Dolomanov, L. J. Bourhis, R. J. Gildea, J. A.-K. Howard and H. Puschmann, OLEX2: A complete structure solution, refinement and analysis program, *J. Appl. Crystallogr.*, 2009, **42**, 339–341.

47 A. L. Spek, Structure validation in chemical crystallography, *Acta Crystallogr., Sect. D: Biol. Crystallogr.*, 2009, **65**, 148–155.

48 J. Tauc, Absorption edge and internal electric fields in amorphous semiconductors, *Mater. Res. Bull.*, 1970, **5**, 721–729.

49 S. J. Clark, M. D. Segall, C. J. Pickard, P. J. Hasnip, M. I.-J. Probert, K. Refson and M. C. Payne, First principles methods using CASTEP, *Z. Kristallogr.*, 2005, **220**, 567–570.

50 J. P. Perdew, K. Burke and M. Ernzerhof, Generalized gradient approximation made simple, *Phys. Rev. Lett.*, 1996, **77**, 3865–3868.

51 K. Liu, H. Fan, P. Ren and C. Yang, Structural, electronic and optical properties of $BiFeO_3$ studied by first-principles, *J. Alloys Compd.*, 2011, **509**, 1901–1905.

52 W. Wang, H. Fan and Y. Ye, Effect of electric field on the structure and piezoelectric properties of poly(vinylidene

fluoride) studied by density functional theory, *Polymer*, 2010, **51**, 3575–3581.

53 M. Mutailipu, M. Zhang, H. P. Wu, Z. H. Yang, Y. H. Shen, J. L. Sun and S. L. Pan, $Ba_3Mg_3(BO_3)_3F_3$ polymorphs with reversible phase transition and high performances as ultraviolet nonlinear optical materials, *Nat. Commun.*, 2018, **9**, 1–10.

54 C. K. Huang and P. F. Kerr, Infrared study of the carbonate minerals, *Am. Mineral.*, 1960, **45**, 311–324.

55 T. T. Tran, J. He, J. M. Rondinelli and P. S. Halasyamani, $RbMgCO_3F$: A New Beryllium-Free Deep-Ultraviolet Nonlinear Optical Material, *J. Am. Chem. Soc.*, 2015, **137**, 10504–10507.

56 M. Q. Gai, Y. Wang, T. H. Tong, Z. H. Yang and S. L. Pan, $ZnIO_3F$: Zinc Iodate Fluoride with Large Birefringence and Wide Band Gap, *Inorg. Chem.*, 2020, **59**, 4172–4175.

57 Q. M. Huang, C. L. Hu, B. P. Yang, Z. Fang, Y. Huang and J. G. Mao, $Ba_2[FeF_4(IO_3)_2]IO_3$: a promising nonlinear optical material achieved by chemical-tailoring-induced structure evolution, *Chem. Commun.*, 2021, **57**, 11525–11528.

58 T. H. Wu, X. X. Jiang, C. Wu, H. Y. Sha, Z. J. Wang, Z. S. Lin, Z. P. Huang, X. F. Long, M. G. Humphrey and C. Zhang, From $Ce(IO_3)_4$ to $CeF_2(IO_3)_2$: fluorinated homovalent substitution simultaneously enhances SHG response and band-gap for mid-infrared nonlinear optics, *J. Mater. Chem. C*, 2021, **9**, 8987–8993.

59 L. J. Sham and M. Schlüter, Density-Functional Theory of the Energy Gap, *Phys. Rev. Lett.*, 1983, **51**, 1888–1891.

60 A. J. Cohen, P. Mori-Sánchez and W. Yang, Fractional charge perspective on the band gap in density-functional theory, *Phys. Rev. B: Condens. Matter Mater. Phys.*, 2008, **77**, 115–123.

61 Y. W. An, Y. Zhong, T. Q. Sun, H. J. Wang, Z. P. Hu, H. D. Liu, S. G. Liu, Y. F. Kong and J. J. Xu, Synthesis, structure and characterization of $M(IO_3)_2(HIO_3)$ (M = Ca, Sr) as new anhydrous alkaline earth metal bis-iodate hydrogeniodate compounds, *Dalton Trans.*, 2019, **48**, 13074–13080.

62 J. Chen, C. L. Hu, F. F. Mao, B. P. Yang, X. H. Zhang and J. G. Mao, REI_5O_{14} (RE = Y and Gd): Promising SHG Materials Featuring the Semicircle-Shaped $I_5O_{14}^{3-}$ Polyiodate Anion, *Angew. Chem., Int. Ed.*, 2019, **58**, 11666–11669.

63 D. E. Zelmon, D. L. Small and D. Jundt, Infrared corrected Sellmeier coefficients for congruently grown lithium niobate and 5 mol% magnesium oxide–doped lithium niobate, *J. Opt. Soc. Am. B*, 1997, **14**, 3319–3322.

64 G. Ghosh, Dispersion-equation coefficients for the refractive index and birefringence of calcite and quartz crystals, *Opt. Commun.*, 1999, **163**, 95–102.

65 G. Q. Zhou, J. Xu, X. D. Chen, H. Y. Zhong, S. T. Wang, K. Xu, P. Z. Deng and F. X. Gan, Growth and spectrum of a novel birefringent α-BaB_2O_4 crystal, *J. Cryst. Growth*, 1998, **191**, 517–519.

